NCAR Manuscript 68-185

An Example of the Nonuniqueness of Weak Solutions Containing Shocks in Fluid Dynamics

Akira Kasahara and David D. Houghton

National Center for Atmospheric Research

Boulder, Colorado 80302

August 1968

ABSTRACT

The system of nonlinear hyperbolic equations of shallow water flow over an obstacle yields different solutions containing discontinuities for the same initial conditions depending upon the form in which the equations are written. Two different solutions are obtained by numerical computations. The results are compared with two different sets of analytical solutions based upon two different formulations of shock conditions. The good agreement between the numerical and analytical results indicates that the nonuniqueness of shock solutions can be demonstrated in the numerical solutions of finite difference equations as well as in the analytical solutions of differential equations.

1. INTRODUCTION

The motions of an incompressible, homogeneous, inviscid, and hydrostatic fluid can be described by the system of "shallow water" equations. Consider one-dimensional "shallow water" flow over an isolated obstacle as shown in Fig. 1. The governing equations may be written as [8]

$$\frac{\partial u}{\partial t} + u\frac{\partial u}{\partial x} + g\frac{\partial \varphi}{\partial x} + g\frac{\partial H}{\partial x} = 0, \tag{1.1}$$

$$\frac{\partial \varphi}{\partial t} + \frac{\partial}{\partial x}(\varphi u) = 0, \tag{1.2}$$

where x and t denote the space and time coordinates; u and φ denote the horizontal velocity and the depth of the fluid; and H is the height of an obstacle above the flat lower boundary. The parameter g denotes the vertical acceleration due to gravity.

The number of equations in the system is equal to the number of unknowns. We may, therefore, expect that appropriate initial and boundary conditions lead to unique behavior without recourse to any further physical principles. This expectation, however, is valid only for the regions of continuous motion. When Eqs. (1.1) and (1.2) are solved for some initial conditions, hydraulic jumps develop [3]. The purpose of this paper is to demonstrate that the solutions of the problem containing shock (or jump) discontinuities are in general not unique even for the same initial conditions. As pointed out by Lax [4], shock solutions associated

with a given system of equations depend on the form in which the equations are written. When the system of equations is solved numerically in finite difference form, the question of nonuniqueness of shock solutions becomes difficult to answer because of the accuracy of the finite difference equations. The example presented in this paper will show clearly that the nonuniqueness of shock solutions can be demonstrated in numerical solutions as well as in analytical solutions of differential equations.

2. SHOCK CONDITIONS

Let us rewrite the system of equations (1.1) and (1.2) in the conservation law form

$$U_t + F_x + B = 0 \tag{2.1}$$

where

$$U = \begin{pmatrix} u \\ \varphi \end{pmatrix}, \quad F = \begin{pmatrix} \frac{u^2}{2} + g\varphi \\ u\varphi \end{pmatrix}, \quad B = \begin{pmatrix} g H_x \\ 0 \end{pmatrix} \tag{2.2}$$

and the subscripts x and t denote differentiation.

U is called a <u>weak solution</u> of Eq. (2.1) with initial value U(x,o) if the integral relation

$$\iint \{W_t U + W_x F - WB\} dx dt + \int W(x,0) U(x,0) dx = 0 \tag{2.3}$$

holds for every test vector W which has continuous first derivatives and which vanishes outside of some bounded region. Eq. (2.3) is obtained by multiplying (2.1) by W and integrating by parts. A weak solution with continuous first derivatives is called a <u>genuine solution</u> [4].

Weak solutions need not be differentiable. If U_1 and U_2 are two genuine solutions of (2.1) whose domains in the x,t plane are separated

by a smooth curve, the two taken together will constitute a weak solution if and only if the slope τ of the separating curve and the value of U_1 and U_2 along the curve satisfy the condition

$$\frac{1}{\tau}(U_2 - U_1) = F(U_2) - F(U_1). \tag{2.4}$$

The inverse of τ, denoted by

$$C = \tau^{-1} \tag{2.5}$$

is called the propagation velocity of the discontinuity [4]. See also [2].

Shock conditions in velocity form. Applying (2.4) and (2.5) to (2.1), the following shock conditions are derived:

$$C = \left(\frac{u_2^2}{2} - \frac{u_1^2}{2} + g\varphi_2 - g\varphi_1\right) / (u_2 - u_1), \tag{2.6}$$

$$C = (u_2\varphi_2 - u_1\varphi_1) / (\varphi_2 - \varphi_1). \tag{2.7}$$

Eliminating u_2 from (2.6) with the use of (2.7), we get

$$C = u_1 \pm \sqrt{\frac{2g\varphi_2^2}{\varphi_1 + \varphi_2}}. \tag{2.8}$$

The proper choice of sign preceding the radical of (2.8) must be determined on the basis of the physical problem under consideration.

Condition (2.7) can be derived from the requirement for the mass continuity through the discontinuity. There is no question about this formulation. Condition (2.8), on the other hand, is slightly different from the usual condition of hydraulic jumps which are discussed, for example, by Rouse [7] and Stoker [8].

In order to derive, based on the theory of weak solutions, the same discontinuity conditions presented by Rouse and Stoker, we must first write the system of equations (1.1) and (1.2) using as the dependent variables momentum and mass instead of velocity and mass. Let us define the momentum by

$$m = u\varphi. \tag{2.9}$$

Multiplying (1.1) and (1.2) by φ and u, respectively, and adding the two resulting equations, it follows that

$$\frac{\partial m}{\partial t} + \frac{\partial}{\partial x}\left(\frac{m^2}{\varphi}\right) + g\varphi\frac{\partial \varphi}{\partial x} + g\varphi\frac{\partial H}{\partial x} = 0. \tag{2.10}$$

The system of equations (2.10) and (1.2) can be put into the following conservation law form

$$V_t + G_x + K = 0, \tag{2.11}$$

where

$$V = \begin{pmatrix} m \\ \varphi \end{pmatrix}, \quad G = \begin{pmatrix} \frac{m^2}{\varphi} + \frac{1}{2} g \varphi^2 \\ m \end{pmatrix}, \quad K = \begin{pmatrix} g \varphi \frac{\partial H}{\partial x} \\ 0 \end{pmatrix}.$$

Shock conditions in momentum form. Applying (2.5) and the equation comparable to (2.4) to (2.11), the following shock conditions are derived using (2.9) in terms of the original dependent variables u and φ:

$$C = \frac{u_2^2 \varphi_2 - u_1^2 \varphi_1 + \frac{1}{2} g (\varphi_2^2 - \varphi_1^2)}{\varphi_2 u_2 - \varphi_1 u_1}, \tag{2.13}$$

$$C = \frac{u_2 \varphi_2 - u_1 \varphi_1}{\varphi_2 - \varphi_1}. \tag{2.14}$$

By using (2.14) to eliminate u_2 from (2.13), we obtain

$$C = u_1 \pm \sqrt{g \frac{\varphi_2}{\varphi_1} \frac{\varphi_2 + \varphi_1}{2}}. \tag{2.15}$$

Again the proper choice of sign preceding the radical of (2.15) must be made on the basis of the physical problem.

Condition (2.14) is identical to (2.7), but condition (2.15) is different from (2.8). Stoker [8] derived (2.15) based upon physical considerations. In order to compare conditions (2.8) and (2.15), let us consider a simple jump situation having on one side a depth φ_1 and zero velocity and on the other a depth φ_2 and a velocity u_2, as shown in Fig. 2. For prescribed values of u_1, φ_1, and φ_2, the propagation velocity of C and u_2 can be determined by solving the system (2.7) and (2.8) or the system (2.14) and (2.15), as given below. In this case, the plus sign was taken both in (2.8) and (2.15).

a. Simple jump conditions in velocity form

$$\left.\begin{aligned} u_2 &= u_1 + (r-1)\sqrt{\frac{2}{1+r}} \times \sqrt{g\varphi_1}, \\ C &= u_1 + r\sqrt{\frac{2}{1+r}} \times \sqrt{g\varphi_1}, \end{aligned}\right\} \qquad (2.16)$$

where

$$r = \varphi_2 / \varphi_1 . \qquad (2.17)$$

b. Simple jump conditions in momentum form

$$\left.\begin{aligned} u_2 &= u_1 + (r-1)\sqrt{\frac{1+r}{2r}} \times \sqrt{g\varphi_1}, \\ C &= u_1 + r\sqrt{\frac{1+r}{2r}} \times \sqrt{g\varphi_1}. \end{aligned}\right\} \qquad (2.18)$$

Figure 3 shows a comparison of cases a and b in which $u_1 = 0$. The abscissa denotes φ_2/φ_1, and the ordinate denotes dimensionless values for $C/\sqrt{g\varphi_1}$ and $u_2/\sqrt{g\varphi_1}$. The solid and dashed lines represent the momentum form (2.18) and velocity form (2.16), respectively. The difference in the values of C and u_2 of the two shock conditions a and b increases with the ratio φ_2/φ_1.

3. NUMERICAL SOLUTIONS

The foregoing simple example clearly shows that the formulation of jump conditions associated with a given system of equations depends on the form in which the equations are written. Now the question is whether weak solutions containing jumps are also different when the same physical problem is solved numerically using different forms of the equations but with the same initial conditions. In order to investigate this question in a fairly complex situation, let us consider the following physical problem related to Fig. 1.

For $t < 0$ and $-\infty < x < \infty$, the fluid is completely at rest, and the height of the free surface, denoted by h_o, is constant. The fluid is impulsively set in motion at $t = 0$ so that for $-\infty < x < \infty$ the fluid has a constant horizontal velocity u_o. The problem is then to determine the subsequent motion of the fluid, This problem was treated both analytically and numerically, using the momentum form of equations (2.11), by Houghton and Kasahara [3].

In this section, we treat the same physical problem numerically using the velocity form of equations (2.1). We then compare the results with solutions based on the momentum form of equations (2.11) and having both identical initial and boundary conditions and space and time increments. We used a numerical scheme developed by Lax and Wendroff [5]. Since the computational procedure has been described by Houghton and Kasahara [3], we shall omit details and present only results here. Note that we use the initial condition $u_o/\sqrt{gh_o} = 0.7$. The ratio of the height of the crest to the initial depth H_c/h_o was set at 0.5.

Figure 4a shows the numerical solutions of velocity and the height of the free surface after 400 time steps where the velocity form of equations (2.1) has been used. The symbol V in the upper right corner indicates the velocity form. Figure 4b is the same as Fig. 4a except that the momentum form (2.11) was used. The symbol M in the upper right corner indicates the momentum form. If we compare Fig. 4a with Fig. 4b, we note marked differences in the positions of the downstream jump. This difference in position of the downstream jump becomes more pronounced after 1000 time steps, as shown in Figs. 5a and 5b.

4. ANALYTICAL SOLUTIONS

As seen from Figs. 4 and 5, the structure of the flow in the neighborhood of the obstacle is independent of time. Houghton and Kasahara [3] have shown that after sufficient time has elapsed, the solution in the neighborhood of the obstacle can be determined by analyzing the steady-state solutions of the relevant equations, taking into account proper jump conditions. In the numerical solutions, the jump is not considered to be an interior boundary but is rather a part of the weak solution [9]. In the analytical solutions, however, the jump is regarded as an interior boundary. Jump conditions are applied to piece together steady state solutions for the purpose of obtaining the asymptotic structure of the flow over an isolated obstacle.

The asymptotic solution for the initial depth h_o, the initial velocity u_o, and a smooth obstacle with a crest height of H_c can be determined by the following ten algebraic equations for the ten quantities of the variables shown in Fig. 6. For the momentum form the ten equations are:

a. Jump conditions on the upstream side of the obstacle

$$C_\ell = \frac{h_o u_o - h_A u_A}{h_o - h_A}\,, \tag{4.1}$$

$$C_\ell = u_o - \sqrt{\frac{g h_A}{h_o}\left(\frac{h_A + h_o}{2}\right)}\,. \tag{4.2}$$

Equation (4.1) comes from (2.14), and Eq. (4.2) (with a minus sign preceding the radical) comes from (2.15).

b. Steady flow over the obstacle

$$\frac{u_c^2}{2g} + \varphi_c + H_c = \frac{u_A^2}{2g} + h_A \,, \tag{4.3}$$

$$u_c \varphi_c = u_A h_A \,, \tag{4.4}$$

$$\frac{u_B^2}{2g} + h_B = \frac{u_A^2}{2g} + h_A \,, \tag{4.5}$$

$$u_B h_B = u_A h_A \,. \tag{4.6}$$

c. Critical condition at the crest of the obstacle

$$u_c = \sqrt{g \varphi_c} \,. \tag{4.7}$$

d. Jump conditions on the downstream side of the obstacle

$$C_r = \frac{h_B u_B - h_x u_x}{h_B - h_x} \,, \tag{4.8}$$

$$C_r = u_B - \sqrt{\frac{g h_x}{h_B}\left(\frac{h_x + h_B}{2}\right)} \,. \tag{4.9}$$

e. Rarefaction condition downstream of the obstacle

$$u_x - 2\sqrt{g h_x} = u_o - 2\sqrt{g h_o} . \tag{4.10}$$

The ten equations are the same for the velocity form except that the two jump conditions, (4.2) and (4.9), are replaced, respectively, by

$$C_\ell = u_o - \sqrt{2g \frac{h_A^2}{(h_o + h_A)}} \tag{4.11}$$

and

$$C_\ell = u_B - \sqrt{2g \frac{h_x^2}{(h_x + h_B)}} . \tag{4.12}$$

Equations (4.11) and (4.12) are based on (2.8) except that the sign preceding the radical is minus. These two sets of ten equations were solved by the method described in the Appendix. As in the numerical computations, we set $u_o/\sqrt{gh_o} = 0.7$ and $H_c/h_o = 0.5$. The results of analytical solutions are compared with those of numerical solutions in Table 1. Values taken from the numerical computations are shown only to the number of significant digits that can be determined from the solutions. Note the good agreement between the numerical and analytical solutions for both the velocity and momentum forms of the equations.

TABLE I

COMPARISON OF ANALYTICAL AND NUMERICAL RESULTS

Asymptotic Quantity	Velocity Form Equations		Momentum Form Equations	
	Analytical Value	Computed Value	Analytical Value	Computed Value
h_A/h_o	1.3710	1.3709	1.3677	1.3676
$u_A/\sqrt{gh_o}$	0.3593	0.3593	0.3579	0.3580
$C_\ell/\sqrt{gh_o}$	-0.5592	-0.555	-0.5724	-0.569
φ_c/h_o	0.6237	0.6236	0.6211	0.6211
$u_c/\sqrt{gh_o}$	0.7897	0.7897	0.7881	0.7883
h_B/h_o	0.3315	0.3314	0.3298	0.3298
$u_B/\sqrt{gh_o}$	1.4860	1.4860	1.4846	1.4846
$C_r/\sqrt{gh_o}$	0.2737	0.28	0.1541	0.15
h_x/h_o	0.9827	0.9826	0.9281	0.928
$u_x/\sqrt{gh_o}$	0.6826	0.6825	0.6268	0.628

5. Conclusions

The excellent agreement between the analytical and numerical solutions for both the velocity form and the momentum form of the equations clearly indicates that the nonuniqueness of weak solutions can be demonstrated in the numerical solutions of finite difference equations as well as in the analytical solutions of differential equations.

This immediately raises the question as to which form of equations is better to use. Since momentum is one of the conservative quantities, it seems to be more natural to use the momentum form of the equations to study hydraulic jumps. Of course, the ultimate test must come from a laboratory experiment. Miller [6] performed a laboratory experiment to measure the propagation velocity of hydraulic jump C moving into still water in a channel (Fig. 2). The jump was generated by a moving piston with the velocity u_2 placed at the left end of the channel. Figure 7a shows the observed flow velocity (in this case the velocity of the piston) as a function of the ratio of the elevation of the water surface behind the jump and the depth of the still water, φ_2/φ_1. Figure 7b shows the observed propagation velocity of the jump C as a function of φ_2/φ_1. The solid lines in Figs. 7a and 7b denote the theoretical curves of u_2 and C for the momentum form as given in (2.18). The dashed lines show the theoretical curves of u_2 and C for the velocity form as given in (2.16). The observed data clearly show agreement with the jump conditions of momentum form.

In a more general problem of hydrodynamic shocks in the flow of a compressible fluid, it is customary to use the system consisting of conservation of mass, momentum, and energy (see, for example, [1]). The

Rankine-Hugoniot shock conditions can be derived for this system if Lax's theory of weak solutions is applied. However, as noted by Courant [2, p. 490], different shock solutions will be obtained for the same physical problem by using the system of equations for conservation of mass, momentum, and entropy.

APPENDIX

SOLUTION OF THE TEN ALGEBRAIC EQUATIONS FOR ASYMPTOTIC CONDITIONS

Since Houghton and Kasahara [3] have not discussed how to solve the ten algebraic equations to determine the asymptotic structure of the flow over the obstacle, we explain here a method of solution.

Equations (4.1) and (4.2) were combined to eliminate C_ℓ and written such that for a given value of h_o, u_o is a function of h_A and u_A. Also (4.4) and (4.7) were used to eliminate u_c and φ_c from (4.3). The result is an expression for H_c as a function of h_A and u_A. Thus, we have two equations for u_o and H_c as functions of h_A and u_A. Note that u_o increases monotonically with increasing h_A and u_A, whereas H_c increases monotonically with increasing h_A but decreasing u_A. Therefore, a simple iteration procedure can be used to find the values of h_A and u_A. With the obtained values of u_A and h_A, C_ℓ, φ_c, and u_c can be computed using (4.1), (4.4), and (4.7).

Elimination of u_B between (4.5) and (4.6) gives a cubic equation of h_B for known values of u_A and h_A. This cubic equation can be reduced to a quadratic equation by assuming that $h_B \neq h_A$ since the symmetrical condition is not acceptable. By solving the quadratic equation, we find

$$h_B = \frac{u_A}{4g}\left[\, u_A + \sqrt{u_A^2 + 8g h_A}\,\right].$$

The solution of u_B can then be found from (4.6) if h_B is known.

Finally, Eqs. (4.8) - (4.10) are solved as follows. u_x is first eliminated from (4.8) using (4.10). We then start with a small initial

guess for h_x and gradually increase the value of h_x until Eqs. (4.9) and (4.10) yield sufficiently close values for C_r. Using this solution of h_x, the solution of u_x can be obtained from (4.10).

The other set of ten equations for the velocity form can be solved similarly.

Acknowledgment. The authors wish to thank Professor Eugene Isaacson, Courant Institute of Mathematical Sciences, New York University, for his useful discussions.

REFERENCES

1. S. Z. BURSTEIN, Am. Inst. Aeronautics and Astronautics J. 2, 2111 (1964).

2. R. COURANT, "Methods of Mathematical Physics," Interscience Publishers, New York (1962).

3. D. D. HOUGHTON and A. KASAHARA, Comm. Pure Appl. Math. 21, 1 (1968).

4. P. D. LAX, Comm. Pure Appl. Math. 7, 159 (1954).

5. P. D. LAX and B. WENDROFF, Comm. Pure Appl. Math. 13, 217 (1960).

6. R. L. MILLER, J. Geophys. Res. 73, 4497 (1968).

7. H. ROUSE, "Fluid Dynamics for Hydraulic Engineers," Dover Publications, New York (1961).

8. J. J. STOKER, "Water Waves," Interscience Publishers, New York (1957).

9. J. VON NEUMANN and R. D. RICHTMYER, J. Appl. Phys. 21, 232 (1950).

FIGURE LEGENDS

Figure 1. A cross section view of shallow water flow over an obstacle.

Figure 2. Simple jump configuration used to compare shock conditions.

Figure 3. Dimensionless flow velocity $u_2/\sqrt{g\varphi_1}$ and jump velocity $C/\sqrt{g\varphi_1}$ for the simple jump configuration shown in Fig. 2. Momentum form results are denoted by solid lines and velocity form results are denoted by dashed lines.

Figure 4a. Numerical solution for the velocity form equations after 400 time steps.

Figure 4b. Same as Fig. 4a but for the momentum form equations.

Figure 5a. Same as Fig. 4a but after 1000 time steps.

Figure 5b. Same as Fig. 4b but after 1000 time steps.

Figure 6. Asymptotic conditions in the vicinity of the obstacle. u_o and h_o are initial conditions. For given H_c, the other ten variables are unknowns determinable by the ten algebraic equations in Section 4.

Figure 7a. Comparison of the experimentally determined jump height φ_2 with theoretical curves as a function of piston velocity u_2. Solid line shows momentum form and dashed line velocity form. The experimental data are given by Miller (1968).

Figure 7b. Comparison of experimentally determined jump velocity C with theoretical curves as a function of jump height φ_2. Solid line shows momentum form and dashed line velocity form. The experimental data are given by Miller (1968).

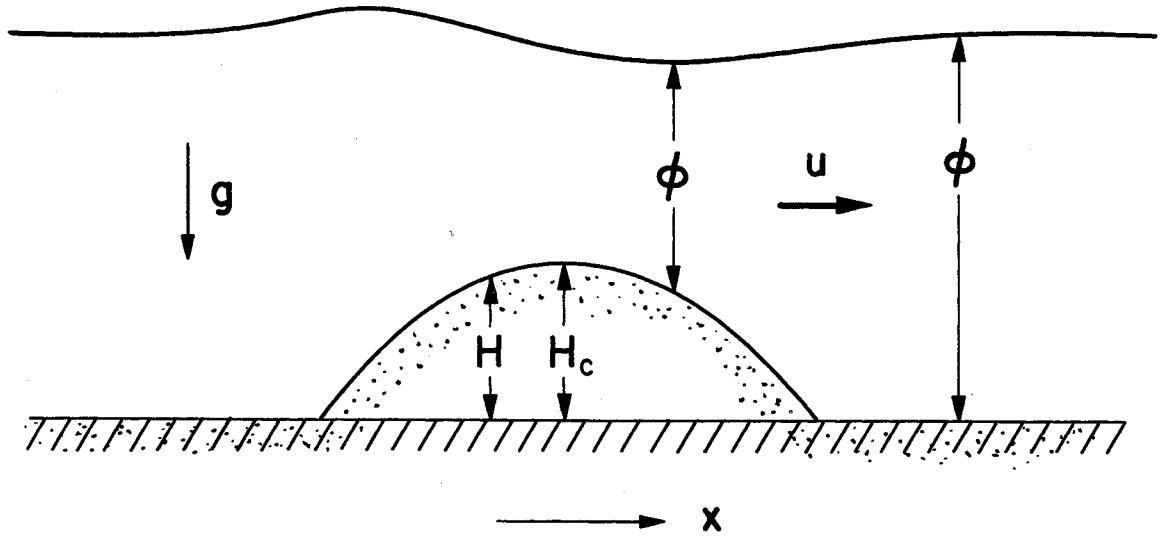

Figure 1. A cross section view of shallow water flow over an obstacle.

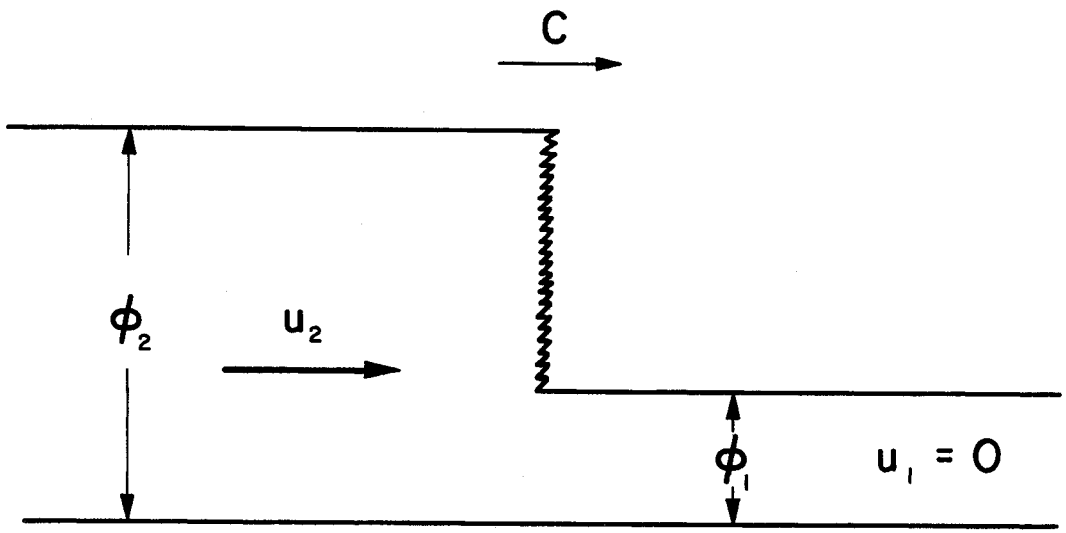

Figure 2. Simple jump configuration used to compare shock conditions.

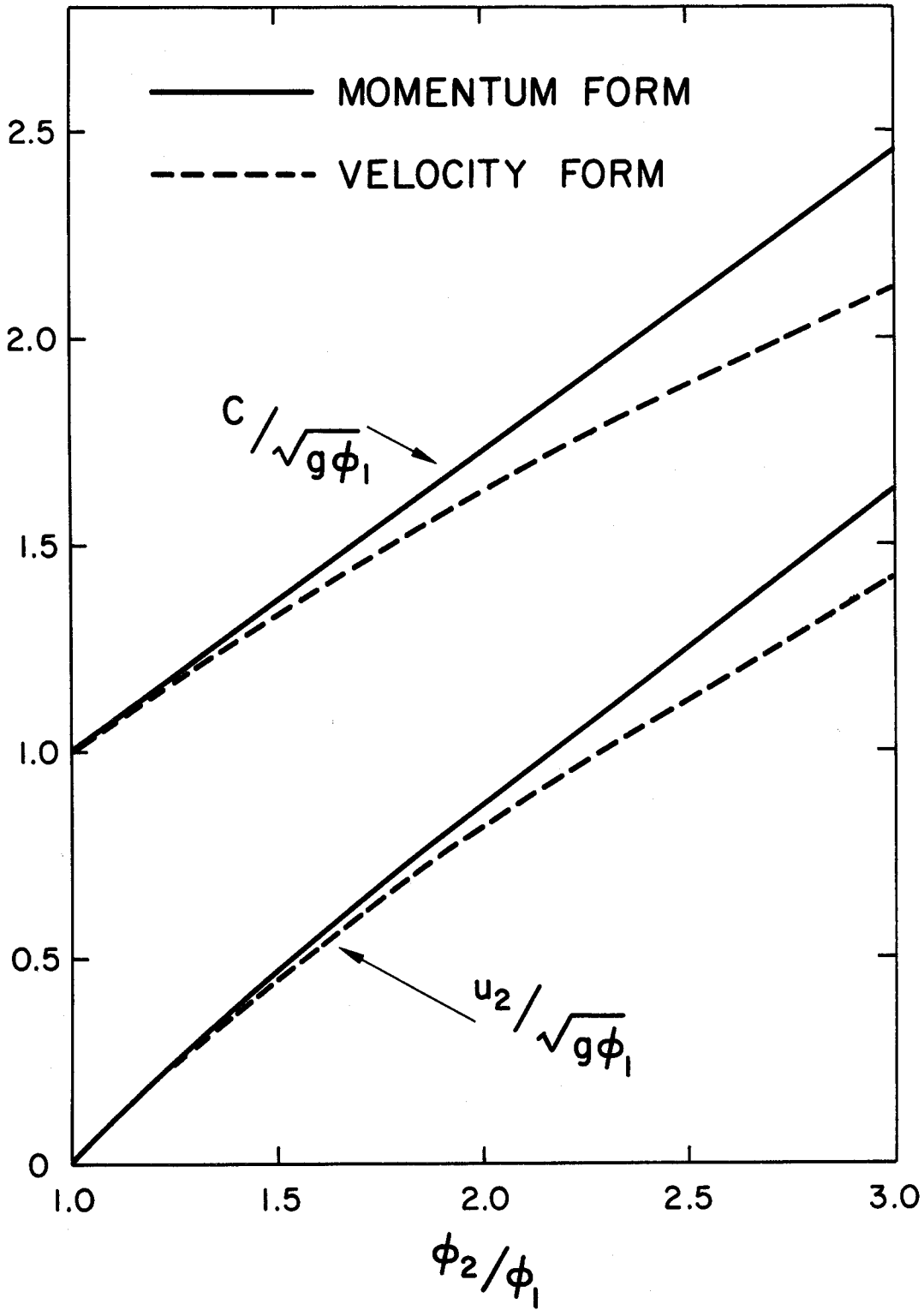

Figure 3. Dimensionless flow velocity $u_2/\sqrt{g\varphi_1}$ and jump velocity $C/\sqrt{g\varphi_1}$ for the simple jump configuration shown in Fig. 2. Momentum form results are denoted by solid lines and velocity form results are denoted by dashed lines.

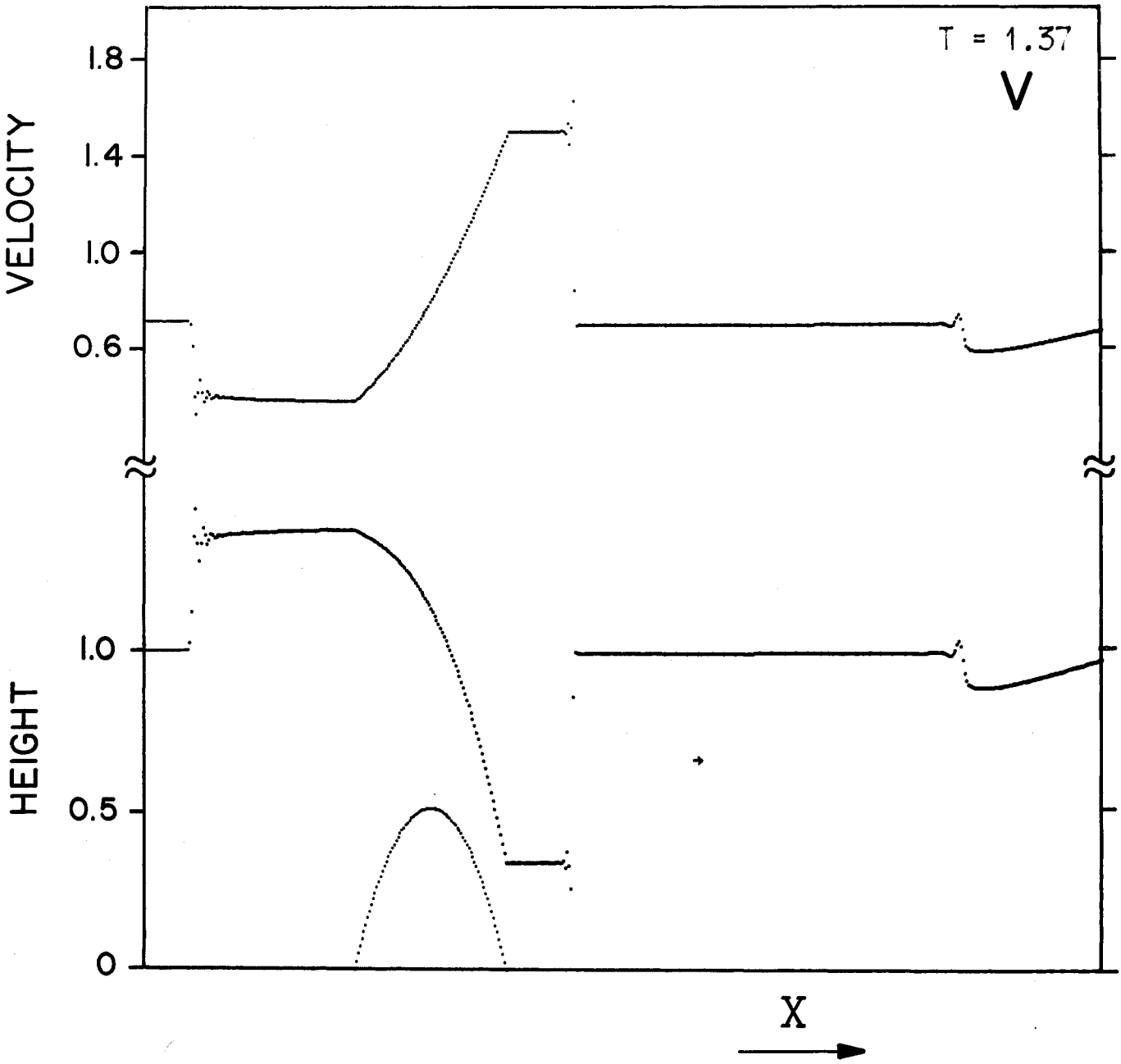

Figure 4a. Numerical solution for the velocity form equations after 400 time steps.

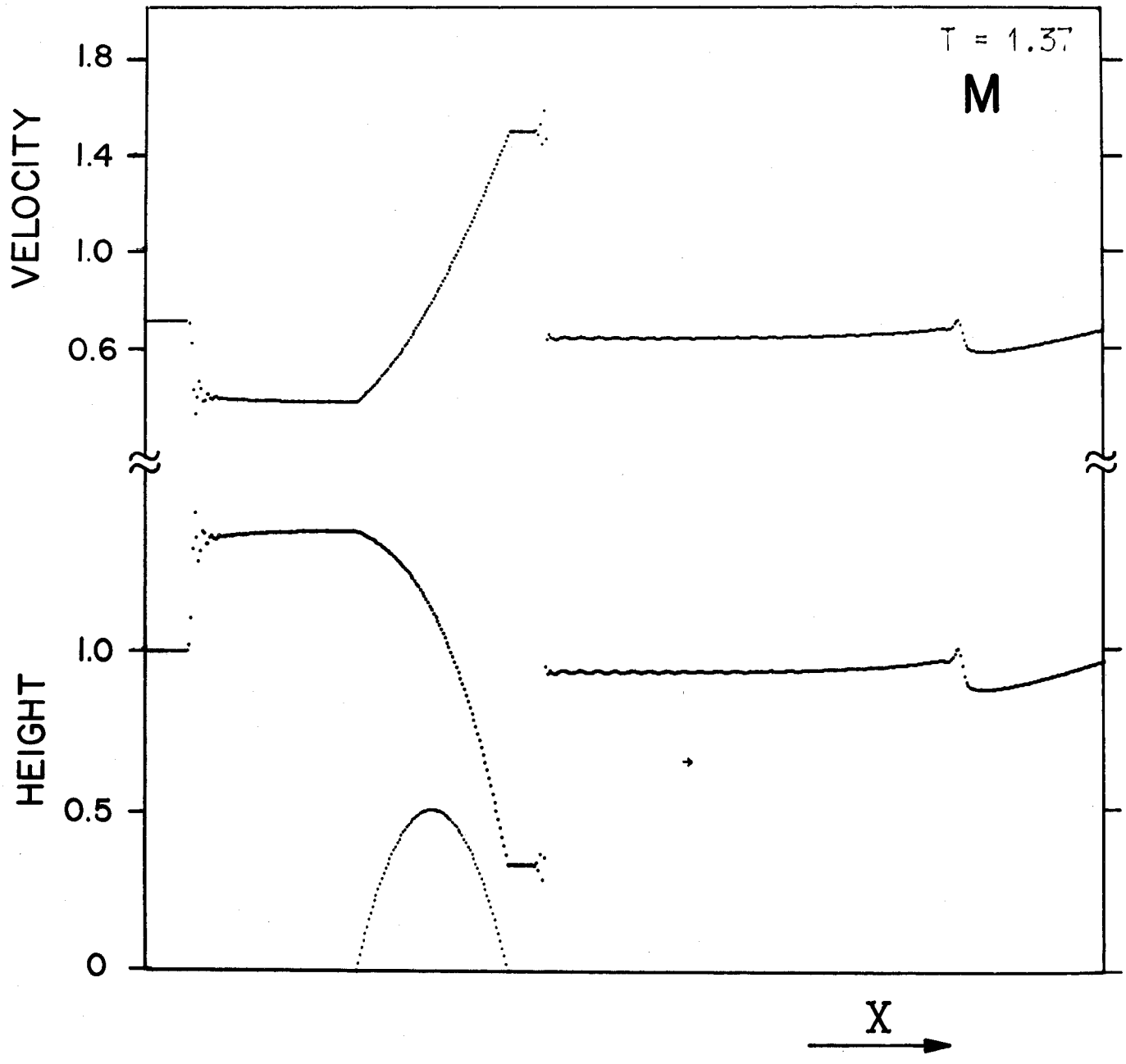

Figure 4b. Same as Fig. 4a but for the momentum form equations.

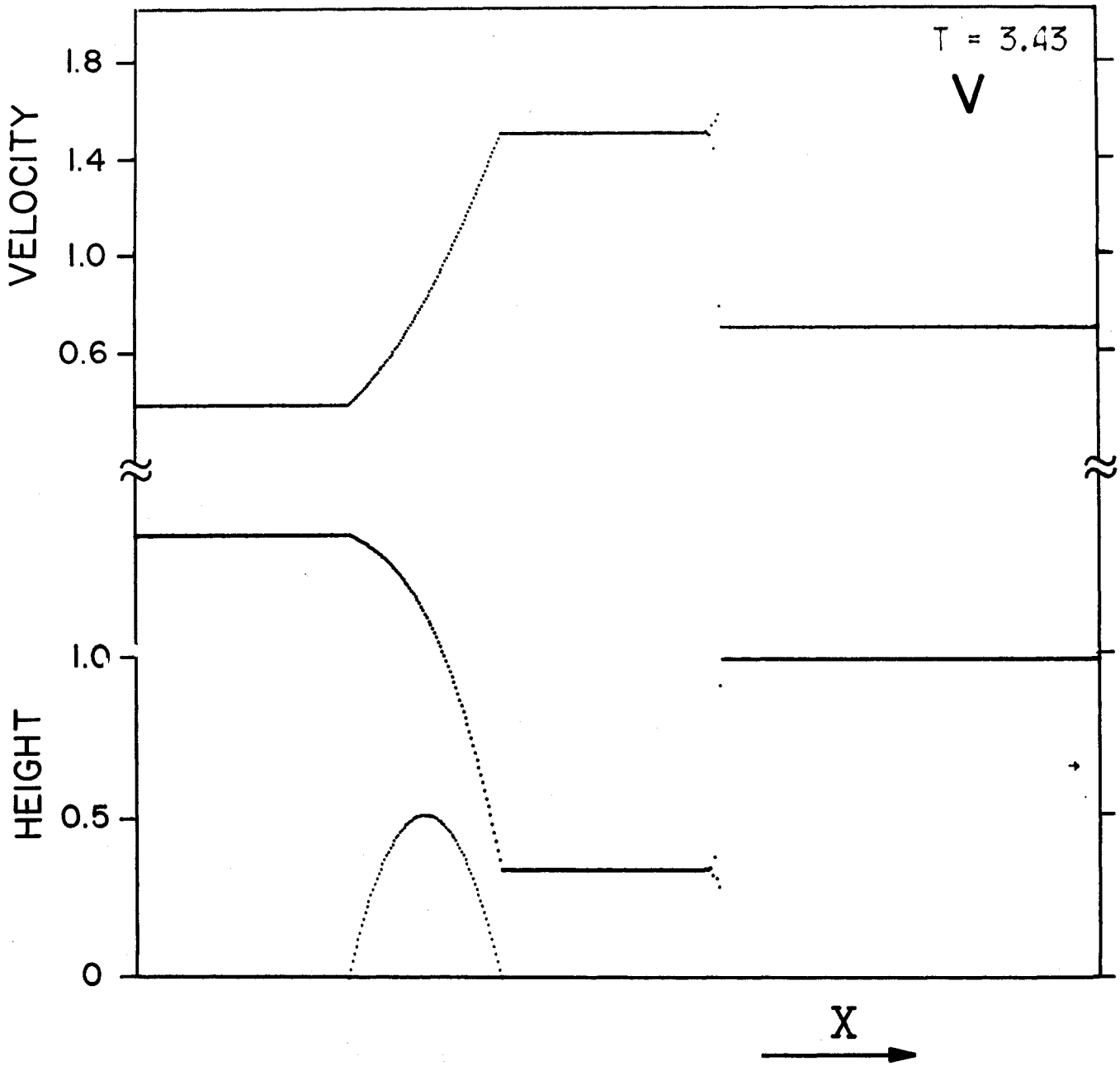

Figure 5a. Same as Fig. 4a but after 1000 time steps.

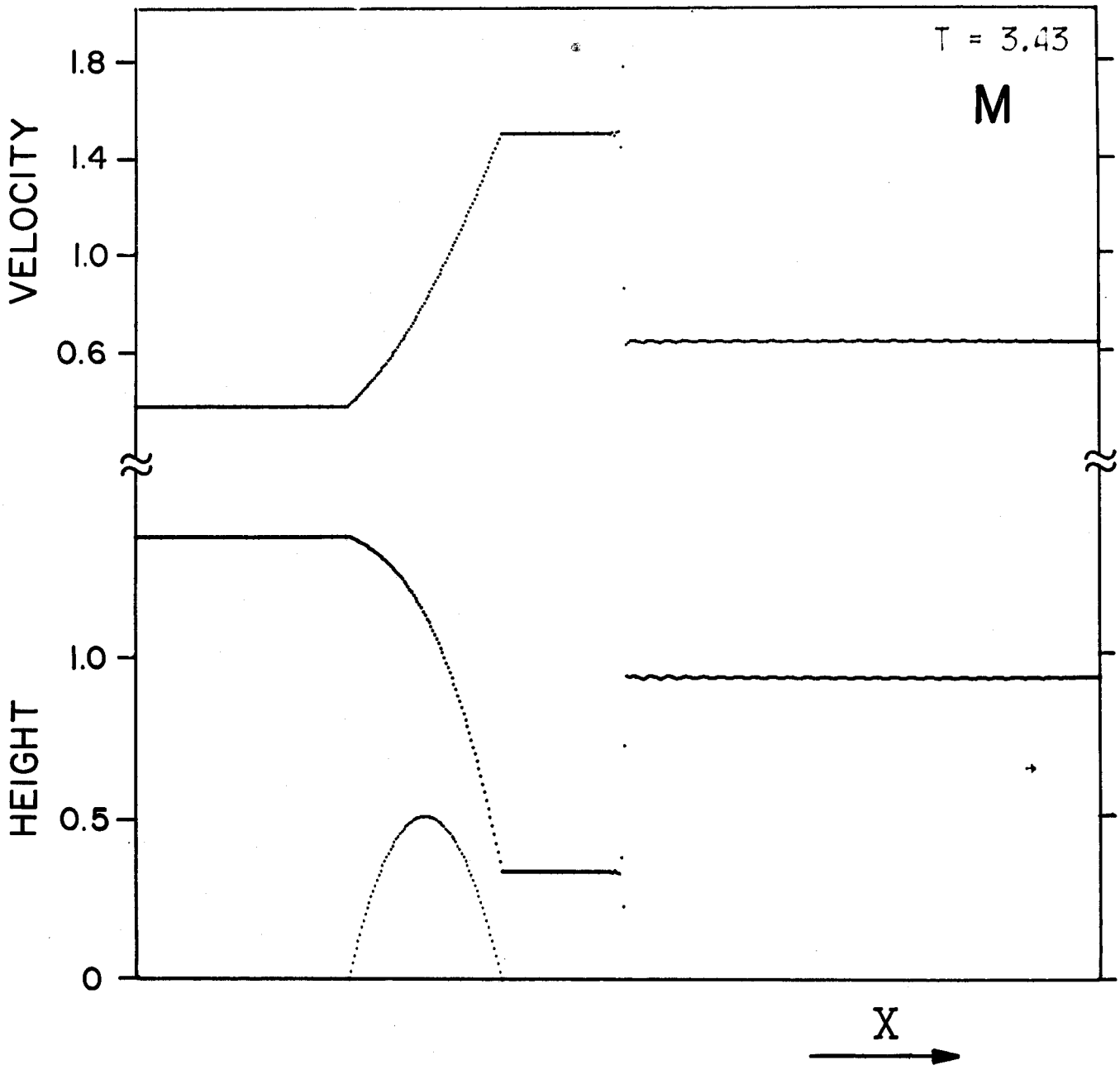

Figure 5b. Same as Fig. 4b but after 1000 time steps.

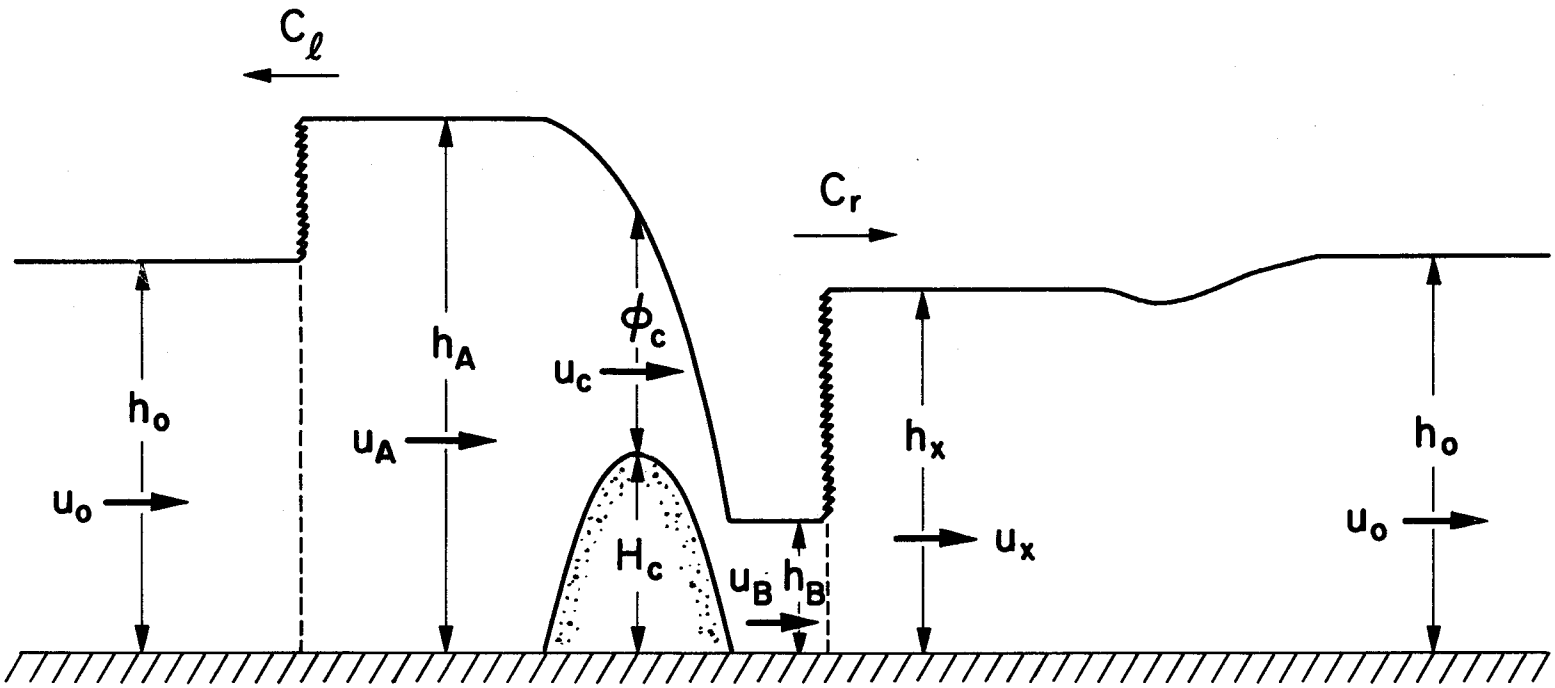

Figure 6. Asymptotic conditions in the vicinity of the obstacle. u_o and h_o are initial conditions. For given H_c, the other ten variables are unknowns determinable by the ten algebraic equations in Section 4.

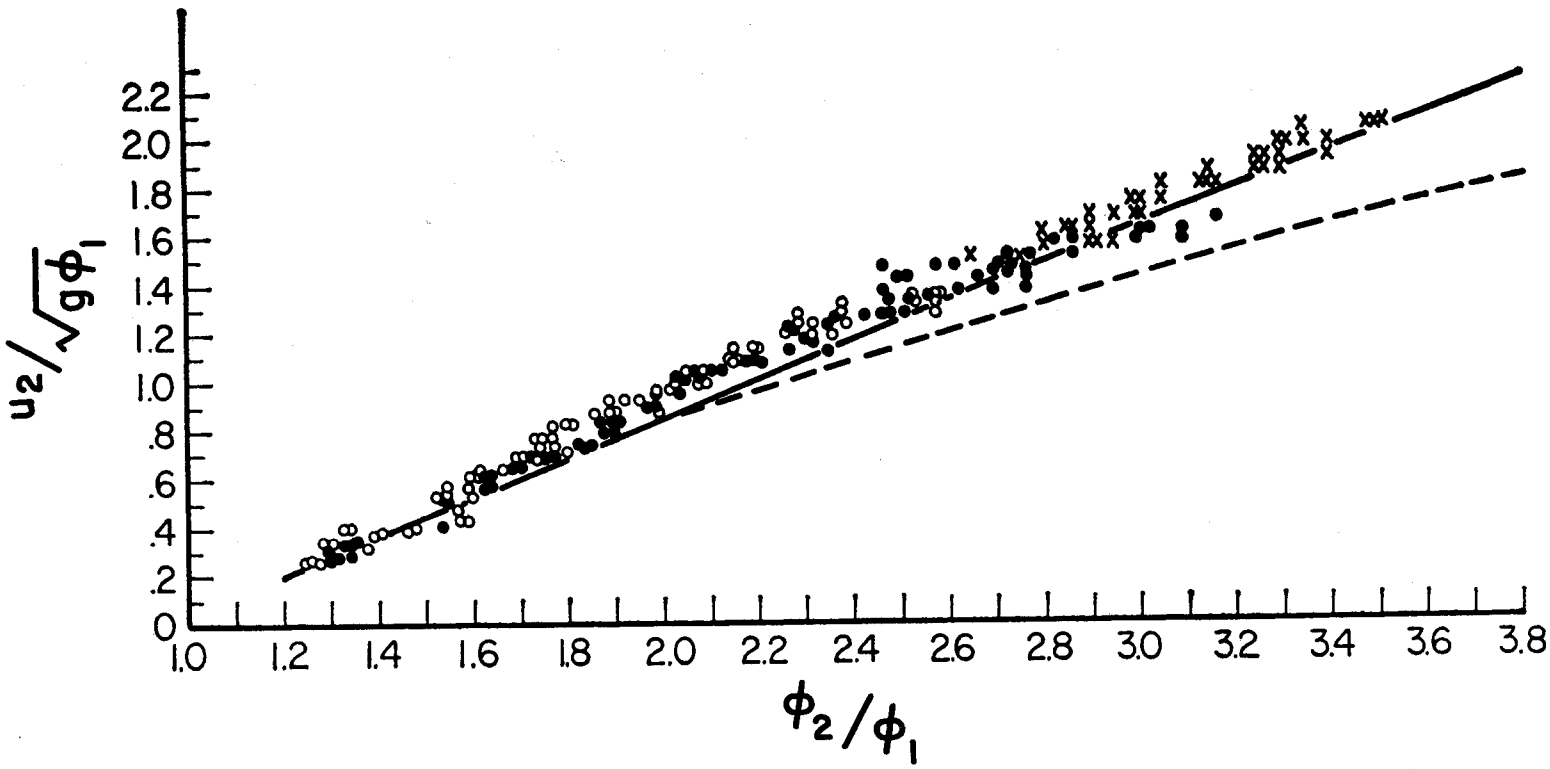

Figure 7a. Comparison of the experimentally determined jump height φ_2 with theoretical curves as a function of piston velocity u_2. Solid line shows momentum form and dashed line velocity form. The experimental data are given by Miller (1968).

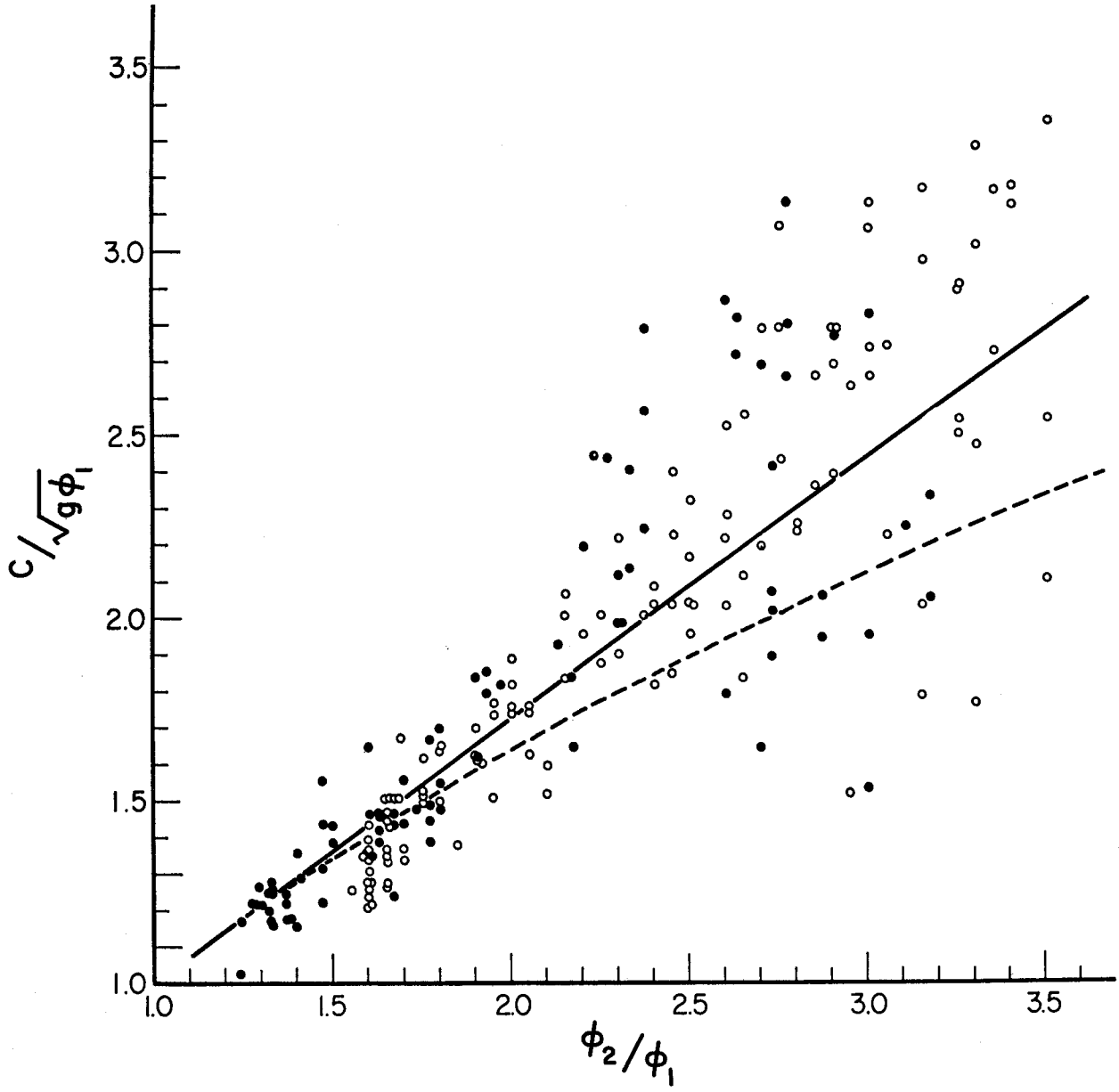

Figure 7b. Comparison of experimentally determined jump velocity C with theoretical curves as a function of jump height φ_2. Solid line shows momentum form and dashed line velocity form. The experimental data are given by Miller (1968).